Published March, 2008

Soil Carbon Saturation: Linking Concept and Measurable Carbon Pools

Catherine E. Stewart*
Natural Resource Ecology Lab.
Colorado State Univ.
Fort Collins, CO 80523-1499

Alain F. Plante
Dep. of Earth and Environmental Science
Univ. of Pennsylvania
Philadelphia, PA 19104-6316

Keith Paustian
Dep. of Soil and Crop Sciences
Colorado State Univ.
Fort Collins, CO 80523

Richard T. Conant
Natural Resource Ecology Lab.
Colorado State Univ.
Fort Collins, CO 80523-1499

Johan Six
Dep. of Plant Sciences
Univ. of California
Davis, CA 95616

The soil C saturation concept suggests a limit to whole soil organic carbon (SOC) accumulation determined by inherent physicochemical characteristics of four soil C pools: unprotected, physically protected, chemically protected, and biochemically protected. Previous attempts to quantify soil C sequestration capacity have focused primarily on silt and clay protection and largely ignored the effects of soil structural protection and biochemical protection. We assessed two contrasting models of SOC accumulation, one with no saturation limit (i.e., linear first-order model) and one with an explicit soil C saturation limit (i.e., C saturation model). We isolated soil fractions corresponding to the C pools (i.e., free particulate organic matter [POM], microaggregate-associated C, silt- and clay-associated C, and nonhydrolyzable C) from eight long-term agroecosystem experiments across the United States and Canada. Due to the composite nature of the physically protected C pool, we fractioned it into mineral- vs. POM-associated C. Within each site, the number of fractions fitting the C saturation model was directly related to maximum SOC content, suggesting that a broad range in SOC content is necessary to evaluate fraction C saturation. The two sites with the greatest SOC range showed C saturation behavior in the chemically, biochemically, and some mineral-associated fractions of the physically protected pool. The unprotected pool and the aggregate-protected POM showed linear, nonsaturating behavior. Evidence of C saturation of chemically and biochemically protected SOC pools was observed at sites far from their theoretical C saturation level, while saturation of aggregate-protected fractions occurred in soils closer to their C saturation level.

Abbreviations: μagg, microaggregate fraction, (53–250 μm); cPOM, coarse unprotected particulate organic matter (>250 μm); CT, conventional tillage; iPOM, microaggregate-protected particulate organic matter (heavier than 1.85 g cm^{-3}, >53 μm in size); H-dClay, hydrolyzable, easily dispersed, clay-sized fraction (acid soluble, <2 μm); H-dSilt, hydrolyzable, easily dispersed, silt-sized fraction (acid soluble, 53–2 μm); H-μClay, hydrolyzable, microaggregate-derived clay-sized fraction (acid soluble, <2 μm); H-μSilt, hydrolyzable, microaggregate-derived silt-sized fraction (acid soluble, 53–2 μm); LF, fine, unprotected POM (lighter than 1.85 g cm^{-3}, 53–250 μm); NH-dClay, nonhydrolyzable, easily dispersed, clay-sized fraction (acid resistant, <2 μm); NH-dSilt, nonhydrolyzable, easily dispersed, silt-sized fraction (acid resistant, 53–2 μm); NH-μClay, nonhydrolyzable, microaggregate-derived clay-sized fraction (acid resistant, < 2 μm); NH-μSilt, nonhydrolyzable, microaggregate-derived silt-sized fraction (acid resistant, 53–2 μm); NT, no-till; POM, particulate organic matter; SOC, soil organic carbon.

Soil C stabilization has been linked to physical soil properties, specifically the amount, reactivity, and surface area of clay minerals. Adsorption to silt- and clay-sized particles protects SOC from decomposition and is controlled by the availability of reactive surface area. Studies of pure clays have found a limit to the stabilization of added organic material (Harter and Stotzky, 1971; Marshman and Marshall, 1981), implying an upper limit to the capacity of soil to protect C by clay adsorption. Adsorption mechanisms have also been used to describe silt + clay SOC protection by Hassink and Whitmore (1997), who explored the influence of soil texture on SOC accumulation by comparing three alternative models of physical protection. Compared with models that incorporated SOC stabilization as a linear function of texture, they found that a model incorporating a finite protective capacity explained the most variance in organic matter additions and losses as a function of soil clay content. This led them to suggest that C accumulation did not necessarily depend on the protective capacity (i.e., texture) of the soil alone, but on the degree to which the protective capacity was already occupied by organic matter.

According to Hassink and Whitmore (1997), the capacity of a whole soil to protect C was based primarily on the silt + clay protective capacity and SOC accumulation in excess of the silt + clay protective capacity would be subject to higher rates of decomposition. Hassink et al. (1997) found that the silt + clay fraction of the 0- to 10-cm layer of their sandy grassland soils contained the same amount of C as their arable counterparts, leading them to conclude that their soils had reached a maximum amount of C associated with the silt and clay fractions. When the protective capacity of the soil had been exceeded, further C additions were not stabilized by the silt + clay fraction and thus C accumulated in the light and intermediate

Soil Sci. Soc. Am. J. 72:379-392
doi:10.2136/sssaj2007.0104
Received 14 Mar. 2007.
*Corresponding author (cstewart@colorado.edu).

macro-organic-matter fractions (>20 μm) (Hassink et al., 1997). Similar to Hassink and Whitmore (1997), Carter et al. (2003) found that sites near or at a C capacity level, defined by silt + clay content, accumulated C only in the POM fraction.

Several researchers have proposed that the capacity of the soil to sequester C is based on more than just the chemical association with silt and clay, being attributable to aggregate protection and biochemical recalcitrance as well. Baldock and Skjemstad (2000) proposed that each mineral matrix had a unique capacity to stabilize organic C depending not only on the presence of mineral surfaces capable of adsorbing organic materials (a protective capacity), but also the chemical nature of the soil mineral fraction, the presence of cations, and the architecture of the soil matrix. They further suggested that the dispersion technique used by Hassink et al. (1997) destroyed aggregate-protected C and potentially redistributed C from POM to silt and clay soil particles. Baldock and Skjemstad (2000) suggested that the constant C content of the silt + clay fraction might be an artifact of the dispersion methodology rather than saturation of adsorption sites and stressed the importance of linking fractionations that isolate both chemical and architectural properties.

Carter (2002) proposed a conceptual model that included a variable capacity related to C input, aggregate stability, and macro-organic matter (OM) in addition to the silt and clay protective capacity. He related the storage capacity of soil to specific soil fractions including the association of SOM with silt + clay particles (<20 μm), microaggregates (20–250 μm), macroaggregates (>250 μm), and sand-sized macro-OM. As SOC concentration increased, C associated with clay and silt reached the protective capacity of the soil, but further C accumulation occurred in aggregate structures and macro-OM as a function of soil type and C inputs (i.e., management).

The whole soil C saturation concept proposed by Six et al. (2002) included not only a silt + clay protected pool (Hassink and Whitmore 1997, Carter 2002), but a microaggregate-protected pool, a biochemically protected pool, and an unprotected pool. In their conceptual model, SOC is stabilized through chemical association with silt and clay particles, physical protection within microaggregates, and biochemical complexity of the organic compounds (Six et al., 2002). A fourth, unprotected C pool is limited by the steady-state balance of C inputs and decomposition, dictated primarily by climate. Theoretically, whole soil C saturation occurs due to the cumulative behavior of these four soil C pools.

Each of the conceptual pools of Six et al. (2002) can be isolated by a simple three-step fractionation procedure using physical, chemical, and density fractionation methods. Our objectives were to evaluate the relative explanatory power of two contrasting models of SOC accumulation, one with no saturation limit (i.e., linear first-order model) and one with an explicit soil C saturation limit (i.e., C saturation model), to assess the mechanisms by which C is stabilized in these soils and to determine values of fraction C saturation capacity when appropriate. To do this, we isolated soil fractions corresponding to the proposed C pools, free POM (unprotected), microaggregate-associated C (physically protected), silt- and clay-associated C (chemically protected), and nonhydrolyzable C (biochemically protected) pools from eight long-term agroecosystem experiments across the United States and Canada. We hypothesized that the chemically protected pool, the aggregate-protected pool, and the biochemically protected pool would saturate at steady state with respect to C due to physicochemical limitations, while the unprotected pool would be determined by the balance of C input and decomposition.

MATERIALS AND METHODS

Field Sites

Soils were sampled between 2002 and 2004 from eight long-term agroecosystem tillage, crop rotation, and fertilizer experiments (Table 1), most of which were described in Paul et al. (1997). At each site, samples were also taken from adjacent grassland or forest soils that, to our knowledge, had never been under agricultural production except for Kentucky and Georgia, where adjacent pasture was sampled. These sites are not part of the original experimental design and thus are "pseudo-replicates."

Akron, Colorado

In 1989, a tillage and crop rotation experiment was established at the Central Great Plains Research Station near Akron, CO, on a Weld silt loam (fine, smectitic, mesic Aridic Argiustoll). Treatments included wheat (*Triticum aestivum* L.)–fallow (WF) under conventional tillage (CT), no-till (NT), and reduced tillage as well as wheat–corn (*Zea mays* L.)–fallow under no-till, and continuous corn under no-till in a randomized complete block design (Follett et al., 2007; Halvorson et al., 2002). The site had been cultivated since 1907 and under tillage trials since 1967 (Halvorson et al., 1997). Sunflower (*Helianthus annuus* L.) was part of the wheat–corn–fallow rotation in 2002. We sampled the WF-CT, WF-NT, and the no-till wheat–corn–sunflower–fallow rotation in 2002. We also sampled a nearby shortgrass prairie that had never been cultivated.

Lexington, Kentucky

A tillage and N fertilization study was initiated in 1970 on a Maury silt loam (fine, mixed, semiactive, mesic Typic Paleudalf). Treatments included two main tillage treatments (NT and CT) with continuous corn (with a rye [*Secale cereal* L.] winter cover crop) at four N fertilization rates. The site was in pasture at least 50 yr before the initiation of experimental treatments. Conventional tillage consisted of moldboard plowing and several subsequent disk harrowings. The experimental design was a split block with four field replicates. Horizontal splits for N and vertical splits for tillage were included in each 11- by 48.8-m block. Further experimental details can be found in Frye and Blevins (1997) and Denef and Six (2005). We sampled the 5.5- by 12.2-m subplots from both tillage treatments within the 85 kg N ha^{-1} fertilizer level in 2002. We also sampled an adjacent bluegrass (*Poa* sp.) pasture.

Hoytville, Ohio

A tillage (NT, minimum tillage, and CT) and crop rotation (continuous corn, corn–soybean [*Glycine max* (L.) Merr.] and corn–oat [*Avena sativa* L.)–meadow) trial was established on a Hoytville silty clay loam (fine, illitic, mesic Mollic Epiaqualf) near Hoytville, OH. Conventional tillage consisted of spring and fall moldboard plowing to 20 to 25 cm as well as one or two 10-cm passes. Before the initiation of the study in 1962, soil was under a corn–oat–meadow rotation for 6 yr. The meadow crop has included mixed grasses and alfalfa (*Medicago sativa* L.) or clover (*Trifolium* sp.) and was cut and removed from the plot. The experimental

design was a factorial randomized complete block design with four field replicates. Plots were 6.4 by 31 m and drainage tiles had been installed (Dick et al., 1997). We sampled the corn–soybean and the corn–oat–meadow rotations under the CT and NT treatments as well as an adjacent forested site that had never been cultivated.

Breton, Alberta, Canada

A tillage, residue management, and N-fertilization study was established on an Orthic Gray Luvisol (Typic Cryoboralf) in 1979 (Nyborg et al., 1995). From 1979 to 1999, the plots were under continuous barley (*Hordeum vulgare* L.) and then changed to a 4-yr barley–canola (*Brassica napus* L. var. *napus*)–wheat–pea (*Pisum sativum* L.) rotation. The treatments were arranged as a randomized block design (10 treatments) with four field replicates (2.8 by 6.9 m). In the spring of 2003, we sampled six treatments that were combinations of tillage (CT vs. NT), straw residue management (removed after harvest vs. left on after harvest), and mineral N fertilization (no fertilizer vs. 112 kg urea-N ha^{-1}). We also sampled an undisturbed adjacent woodlot that had never been cultivated. Further experimental information and soil fraction data are described in Nyborg et al. (1995) and Plante et al. (2006c).

Swift Current, Saskatchewan, Canada

Crop rotation (fallow–spring wheat) and tillage (NT and CT) treatments were established at the Swift Current Agriculture Canada Research Centre on a Swinton silt loam (Aridic Boroll). The site had been cultivated for 70 to 80 yr in a fallow–spring wheat rotation before the initiation of the experiment in 1981. Conventional tillage of continuous wheat consisted of a preseeding tillage using a heavy-duty sweep cultivator with an attached rodweeder and the CT fallow treatment used a heavy-duty cultivator an average of 2.5 passes with occasional rodweeding. Treatments consisted of a randomized complete block design (15 by 76 m) with four field replicates and all phases of the rotation present each year (Campbell et al., 1995). We sampled both tillage treatments as well as a nearby prairie that had never been cultivated in spring 2002.

Scott, Saskatchewan, Canada

A tillage and crop rotation experiment was initiated in 1978 at the Agriculture Canada Experimental Farm in Scott, SK,

Table 1. Site characteristics of the eight long-term agroecosystem experiments sampled.

Site	Location	Experiment initiated	Soil type	Sand	Silt	Clay	Treatments†	0–5-cm average SOC‡	5–20-cm average SOC
				%				g C kg^{-1} soil	
Akron, CO	40°09′ N, 103°09′ W	1989	Aridic Paleustoll	32	41	27	Grass	21.3 ± 0.9	10.6 ± 0.5
							NT wheat–fallow	8.2 ± 0.5	6.1 ± 0.2
							CT wheat–fallow	8.9 ± 0.8	6.4 ± 0.5
							NT wheat–millet–sunflower–fallow	8.9 ± 0.7	7.1 ± 0.3
Lexington, KY	38°07′ N, 84°29′ W	1970	Typic Paleudalf	5	68	27	Grass	28.2 ± 2.4	14.5 ± 0.7
							NT	25.0 ± 1.1	14.2 ± 0.5
							CT	13.2 ± 0.6	13.0 ± 0.8
Hoytville, OH	41°00′ N, 84°00′ W	1962	Mollic Ochraqualf	19	39	42	Forest	70.5 ± 2.0	39.6 ± 2.2
							NT soybean	29.2 ± 0.3	18.6 ± 0.4
							CT soybean	17.1 ± 0.2	17.0 ± 0.2
							NT oat	39.6 ± 1.6	21.5 ± 0.7
							CT oat	18.0 ± 0.5	18.1 ± 0.3
Breton, AB, Canada	53°07′ N 114°28′ W	1979	Typic Cryoboralf	31	39	30	Forest	69.3 ± 1.3	15.6 ± 0.7
							NT, NS, no N	14.0 ± 0.7	11.4 ± 1.3
							CT, NS, no N	13.1 ± 0.2	8.2 ± 0.4
							NT, straw, N	21.4 ± 1.2	12.1 ± 1.9
							CT, straw, N	19.0 ± 0.9	11.9 ± 2.1
Swift Current, SK, Canada	50°17′ N, 107°48′ W	1981	Aridic Haploboroll	26	47	27	Grass	35.4 ± 3.5	25.9 ± 4.9
							NT	23.0 ± 1.0	14.1 ± 1.2
							CT	19.8 ± 1.0	13.2 ± 0.6
Scott, SK, Canada	52°22′ N, 108°50′ W	1978	Typic Borroll	28	44	28	Grass	73.5 ± 7.6	18.8 ± 1.5
							NT	38.8 ± 1.8	22.3 ± 2.0
							CT	35.5 ± 2.1	19.8 ± 2.0
Stewart Valley, SK, Canada	50°17′ N, 107°48′ W	1982	Aridic Haploboroll	20	35	45	Grass	30.3 ± 1.8	19.1 ± 0.7
							NT	20.7 ± 0.8	13.6 ± 0.8
							CT	18.0 ± 0.4	15.2 ± 1.2
Watkinsville, GA	33°54′ N, 83°24′ W	1991	Typic Kanhapludult	69	12	19	Grass	29.4 ± 1.8	7.1 ± 0.7
							NT, N	15.6 ± 0.4	5.1 ± 0.2
							CT, N	11.8 ± 1.3	6.6 ± 0.7

† NT, no-till; CT, conventional tillage; NS, no straw.

‡ Mean and standard errors of soil organic carbon (SOC).

on an Elstow clay loam (Typic Boroll). Treatments included a continuous wheat–flax (*Linum usitatissimum* L.)–wheat and a 3-yr fallow–flax–wheat. The study was a split-plot, randomized complete block design with four field replicates. Plots were 15 by 94 m. Conventional tillage was done with a cultivator with either spikes or sweeps in late fall and harrow disking or rodweeding before seeding in the spring. Tillage fallow was maintained with an average of three passes with a harrow and two with a rodweeder. Further experimental details may be found in Brandt (1992). We sampled the tillage experiment in 2002 as well as a nearby shortgrass prairie that had never been cultivated.

Stewart Valley, Saskatchewan, Canada

Near Stewart Valley, SK, a tillage and crop rotation experiment was established on Hatton fine sandy loam (Aridic Boroll). Before the initiation of the experiment in 1982, the site was cultivated for 70 to 80 yr in a 2- to 3-yr fallow–cereal rotation. Crop rotations included fallow–spring wheat and continuous wheat. Tillage treatments were NT, minimum tillage, and CT (Campbell et al., 1996). We sampled the CT and NT treatments in the continuous wheat rotation with N and P fertilizer, as well as an adjacent shortgrass prairie site that had never been cultivated in the spring of 2002.

Watkinsville, Georgia

Near Watkinsville, GA, a tillage experiment was initiated in 1991 on a Cecil sandy loam (clayey, kaolinitic, thermic Typic Kanhapludult). Runoff collectors and drainage systems were installed to monitor water quality. From 1991 to 1994, both CT and NT treatments were under corn–rye–fallow rotation and from 1994 to 2002, cotton (*Gossypium hirsutum* L.)–wheat or cotton–rye rotations were planted. The site was cultivated 10 yr before the initiation of the experiment with cereal–wheat–fallow rotations. The experimental design was a randomized complete block design of tillage (NT and CT) and N fertilization treatments with three field replicates (10 by 30 m). Conventional tillage consisted of 30-cm-deep chisel plowing, one to two subsequent passes of 20-cm-deep disk harrowing, and finally, a disking to 8 cm. Nitrogen fertilization rates were 60 kg ha^{-1} available N in the form of either NH_4NO_3 or poultry litter (58 kg ha^{-1}, based on dry weight) (Endale et al., 2002). We sampled the CT and NT under a corn–rye rotation fertilized with NH_4NO_3 in spring 2002. We also sampled a nearby grass site that had been under Bermuda grass [*Cynodon dactylon* (L.) Pers.] for 40 yr.

Field Sampling

Between three and 10 surface cores (0–20 cm) were taken and separated into 0- to 5- and 5- to 20-cm depth increments in the field. Litter layers were removed before sampling. Samples were packaged to remain cool and uncompacted during transport to the laboratory. Large rocks, recognizable surface litter, and root material were removed as samples were gently broken by hand and passed through an 8-mm sieve. Soil cores were composited by field replicate, air dried, passed through a 2-mm sieve, and stored at room temperature until further analysis. Depth increments were pretreated, fractionated, and analyzed separately, and were included in all subsequent statistical analyses as individuals to increase the range of SOC concentrations in the study.

Soil texture was determined using a modified version of the standard hydrometer method, without removal of carbonates or organic matter (Gee and Bauder, 1986), on a 30-g subsample dispersed by shaking the soil for 18 h in 100 mL of 5 g L^{-1} sodium hexametaphosphate solution. Total sand contents were determined by sieving (53 μm) and clay contents were measured by the 2-h hydrometer method. Silt contents were determined by difference.

Soil Fractionation

Separation of the various C pools was accomplished by a combination of physical, chemical, and density fractionation techniques in a simple, three-step process (Fig. 1) detailed by Six et al. (2002) and Plante et al. (2006b). The first step was the partial dispersion and physical fractionation of the soil to obtain three size fractions: >250 μm (coarse unprotected particulate organic matter, cPOM), 53–250 μm (microaggregate fraction, μagg), and <53 μm (easily dispersed silt and clay, dSilt and dClay). Physical fractionation was accomplished by fractionating air-dried,

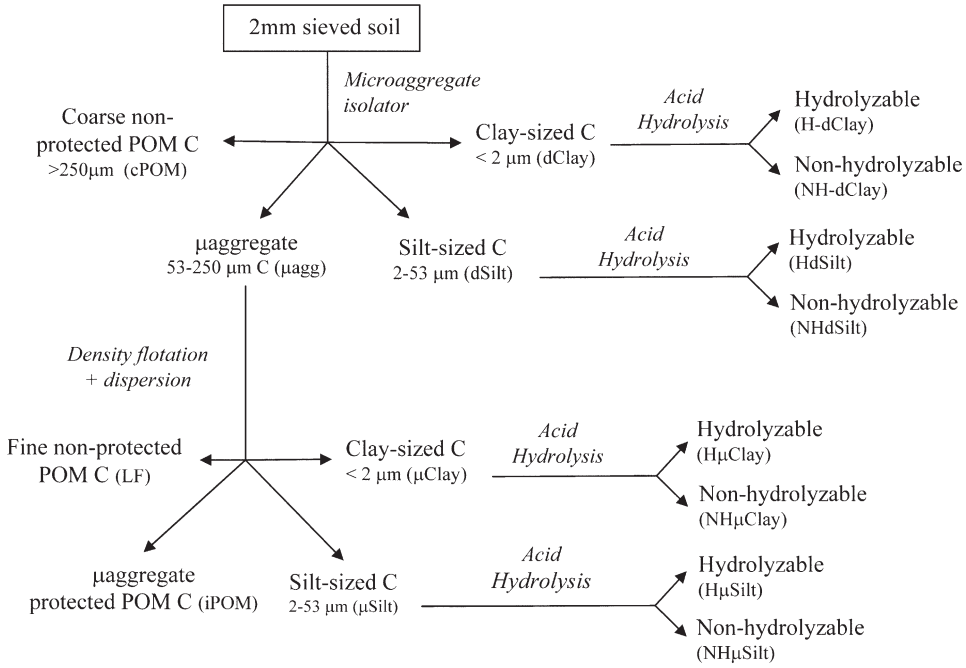

Fig. 1. A three-step soil fraction scheme to isolate the C pools based on physical, chemical, and biochemical protection mechanisms (modified from Six et al., 2002). These fractions are cPOM, coarse unprotected particulate organic matter (>250 μm); μagg, microaggregate fraction (53–250 μm); LF, fine unprotected POM (lighter than 1.85 g cm^{-3}, 53–250 μm); iPOM, microaggregate-protected POM (heavier than 1.85 g cm^{-3}, >53 μm in size); NH-dSilt, nonhydrolyzable, easily dispersed, silt-sized fraction (acid resistant, 53–2 μm); NH-dClay, nonhydrolyzable, easily dispersed, clay-sized fraction (acid resistant, <2 μm); NH-μSilt, nonhydrolyzable microaggregate-derived silt-sized fraction (acid resistant, 53–2 μm); NH-μClay, nonhydrolyzable microaggregate-derived clay-sized fraction (acid resistant, <2 μm); H-dSilt, hydrolyzable, easily dispersed, silt-sized fraction (acid soluble, 53–2 μm); H-dClay, hydrolyzable, easily dispersed, clay-sized fraction (acid soluble, <2 μm); H-μSilt, hydrolyzable microaggregate-derived silt-sized fraction (acid soluble, 53–2 μm); H-μClay, hydrolyzable microaggregate-derived clay-sized fraction (acid soluble, <2 μm).

2-mm sieved soil in the microaggregate isolator described by Six et al. (2000). The microaggregate isolator dispersed the >2-mm soil with 50 glass beads in running water over a 250-μm sieve to flush microaggregates and finer particles through the 250-μm mesh screen. Material >250 μm (cPOM plus sand) remained on the sieve. Microaggregates were collected on a 53-μm sieve that was subsequently wet sieved by hand for 50 strokes in 2 min (Elliott, 1986) to separate the easily dispersed silt- and clay-sized fractions from the water-stable microaggregates. The resulting suspension was centrifuged to separate the easily dispersed silt- and clay-sized fractions. Fractions were oven dried (60°C) and weighed.

The second step involved further fractionation of the microaggregate fraction isolated in the first step (Six et al., 2000, Plante et al., 2006a). Density flotation using 1.85 g cm^{-3} sodium polytungstate was used to isolate fine, unprotected POM (LF) (Six et al., 1998). After removing the fine unprotected POM, the heavy fraction was dispersed overnight by shaking with 12 glass beads and passed through a 53-μm sieve, separating the microaggregate-protected POM (>53 μm in size, iPOM) and the microaggregate-derived silt- and clay-sized fractions (μSilt and μClay).

The third step involved acid hydrolysis of each of the isolated silt- and clay-sized fractions. The silt- and clay-sized fractions from both the density floatation (μSilt and μClay) and the initial dispersion and physical fractionation (dSilt and dClay) were subjected to acid hydrolysis as described in Plante et al. (2006a). Acid hydrolysis consisted of refluxing at 95°C for 16 h in 6 mol L^{-1} HCl. After refluxing, the suspension was filtered and washed with deionized water over a glass-fiber filter. Residues were oven dried at 60°C, weighed, and analyzed for organic C content. These represented the nonhydrolyzable C fractions (NH-dSilt, NH-dClay, NH-μSilt, and NH-μClay). The hydrolyzable C fractions (H-dSilt, H-dClay, H-μSilt, and H-μClay) were determined by difference between the total organic C content of the whole fractions and the C contents of the nonhydrolyzable fractions.

This fractionation scheme is based on the assumed link between the isolated fractions and the protection mechanisms involved in the stabilization of organic C within that pool, as described by Six et al. (2002). The unprotected C pool consists of the cPOM fraction isolated during the first dispersion step and the LF fraction isolated during the second fractionation step. The physically protected C pool consists of the μagg fraction as a whole and the particulate organic matter occluded within it (iPOM). The chemically protected C pool corresponds to the hydrolyzable portion of the silt- and clay-sized fractions isolated during the initial dispersion (H-dSilt and H-dClay). Carbon is stabilized in these fractions through mineral–organic matter bindings, dictated by both the texture and the mineralogy of the soil. The biochemically protected C pool corresponds to the nonhydrolyzable C remaining in the silt- and clay-sized fractions after acid hydrolysis (NH-dSilt and NH-dClay).

Due to the stepwise fractionation procedure, the physically protected pool (μagg) consisted of isolated fractions with multiple protection mechanisms. We distinguished between pure physical protection of POM (iPOM) and the mineral-associated fractions. Carbon stabilized in the mineral-associated fractions was described either as being chemically protected (H-μSilt and H-μClay) or biochemically protected (NH-μSilt and NH-μClay). Consequently, the microaggregate-derived nonhydrolyzable fractions (NH-μSilt and NH-μClay) represent both the biochemical and physical protection mechanisms. Similarly, the hydrolyzable microaggregate-derived silt and clay fractions (H-μSilt and H-μClay) capture both the chemical and physical protection mechanisms.

Carbon Analyses

Carbon contents for all fractions except fine unprotected POM were measured using a LECO CHN-1000 analyzer (Leco Corp., St. Joseph, MI). Fine unprotected POM was measured on a Carlo Erba NA 1500 CN analyzer (Carlo-Erba Instrumenzione, Milan) due to smaller sample size. Soil carbonates were determined by a modified pressure transducer method described by Sherrod et al. (2002).

Theory Underlying Models

Soil C saturation is characterized by an asymptotic relationship between whole SOC across increasing C inputs at steady state (Six et al., 2002; Stewart et al., 2007). Soil C inputs cannot be used as the independent variable in an analysis of fraction C, however, because of the difficulty in fully assessing how soil C inputs are distributed to the individual soil fractions, and how to properly distinguish between fresh C inputs to a fraction and C transfers between fractions. Due to the differing rates of decomposition and subsequent incorporation of C input into various C pools, those pools with slow turnover times do not reflect influences from field-level treatments across shorter time scales. If we were to examine fraction C with C inputs as the independent variable, differences in decomposition as a result of field treatments (i.e., tillage) would produce varying levels of whole SOC, confounding the relationship of fraction C and C inputs. Therefore, when examining soil fractions, it is crucial to express soil fraction C across a normalized scale. We used whole SOC concentration, as a balance between C input and decomposition, to normalize across treatments and be a more appropriate measure of C accumulation.

We demonstrate that at steady state, the same characteristics of linearity for nonsaturating soils and asymptotic behavior for C-saturating soils hold for either C input or SOC concentration as independent variables (see Appendix). In other words, a whole soil that shows a linear increase in C with respect to C inputs (at steady state) will also exhibit linearity between SOC concentration of the whole soil and SOC concentrations of the constituent C fractions. A whole soil accumulating C asymptotically with respect to C inputs (under C saturation) will exhibit an asymptotic relationship between whole SOC concentration and SOC concentration for one (or more) fractions and an exponential relationship for the other fractions. Since the SOC of these fractions must sum to whole SOC, as one fraction saturates, the relative proportion of the other fraction must increase exponentially to compensate as whole SOC increases. Therefore, an increasing exponential behavior for the relative proportion of total C within a fraction is not contradictory to C saturation (see Appendix).

Thus, we used total SOC as a proxy for C input to determine if fraction SOC was influenced by C saturation. A soil fraction exhibiting a linear relationship between whole SOC and fraction SOC is interpreted as not being influenced by C saturation, while a fraction exhibiting an asymptotic relationship shows evidence for C saturation. Since we are concerned only with the general relationship between SOC and fraction C, simple mathematical expressions of both relationships will suffice.

For a model with first-order decomposition kinetics, we show that a soil fraction C (C_f^*) is directly proportional to whole SOC concentration (C_t^*) at steady state:

$$C_f^* = \omega C_t^* + R \quad [1]$$

(see Appendix). We added an intercept term, R, to account for residual SOC not affected during the course of the experiment (Stewart et al., 2007).

In contrast to the linear model, a model including a simple saturation term can be represented by a simple asymptotic equation between soil fraction C (C_f^*) and whole SOC concentration (C_t^*) at steady state:

$$C_f^* = \frac{C_t^*}{\xi + (C_t^*/\Gamma)} \quad [2]$$

(see Appendix). As a soil fraction approaches a maximum value (Γ), the proportion of total C stabilized by physicochemical mechanisms is reduced by the amount of SOC present (C_t^*) to the maximum C level of the fraction (Γ), i.e., the SOC stabilization efficiency decreases. This generalized equation does not explicitly address mechanisms of C saturation, but it does allow a simple description of C saturation behavior of fraction C concentration with respect to whole SOC concentration and provides an explicit estimate of the fraction C saturation limit (Γ). The remaining whole SOC that is not stabilized within the fraction is either lost through respiration or stabilized in other soil fractions. Although we examined each fraction for C saturation behavior, we made no attempt to examine C saturation of the whole soil.

We used long-term agricultural experiments to assess soil fraction C saturation and assumed that the tillage, fertilization, and residue management treatments have reached steady state. The sites selected for inclusion in our analysis have been under continuous cultivation for 75 to 100 yr, and the majority of the current experimental management treatment designs have been in place for at least 20 yr (Table 1).

The linear and C-saturation models were fit to each site's fraction data and the combined data of each fraction using PROC REG and PROC NLIN in SAS/STAT (SAS Institute, Cary, NC). The criterion for model fit was R^2 value calculated for both using corrected sum of squares. Parameter estimates for Γ were compared using confidence limits of the estimates from PROC NLIN, as multiple model fits for each site were unavailable. Differences between estimates of Γ within a site were considered significant if their confidence intervals did not overlap.

RESULTS

Individual Sites

Within each site, the range in whole SOC concentrations was 18 to 77 g C kg^{-1} soil (Table 1). The broadest range in SOC concentrations was in the OH, AB, and Scott, SK (SCO) samples due to the high SOC concentrations in the forest (OH and AB) and prairie (SCO). The other five sites had a SOC range <31 g C kg^{-1} soil. Both linear and saturation model fits of the data were generally good, with R^2 in most cases >0.75; however, model fits of the Stewart Valley (SV) fractions were generally poor (0.01–0.36 R^2; data not shown).

The fractions of the chemically protected pool (H-μSilt and H-μClay) and biochemically protected pool (NH-dSilt and NH-dClay) were best fit with the saturation model at half or more sites (Table 2). The fractions representing the unprotected SOC pool (cPOM and LF) at most sites were better fit with the linear model than the C saturation model. As a whole, the μagg fraction linear best-fit models were only slightly better than the saturation model and four sites showed no difference between models (Table 2). This reflects the composite behavior of the μagg fraction (iPOM + H-μSilt + H-μClay + NH-μSilt + NH-μClay), with all sites having linear best fits of the iPOM fraction and the sites split between C saturation and linear model best fits in the aggregate-associated mineral fractions (H-μSilt, H-μClay, NH-μSilt, and NH-μClay).

Table 2. Number of sites out of eight for which the relationship between whole soil organic carbon (SOC) and fraction organic C concentrations are best fit by the linear or C saturation models based on the greatest R^2. The microaggregate (μagg) fraction is comprised of microaggregate-protected particulate organic matter (iPOM) and mineral-associated fractions (nonhydrolyzable = NH-μSilt and NH-μClay and hydrolyzable = H-μSilt and H-μClay).

SOC Pool	Isolated fraction†	Linear model best fit	C saturation model best fit
Unprotected	cPOM	8	0
	LF	6	2
Physical	μagg‡	3	1
	iPOM	8	0
Physical–biochemical	NH-μSilt	4	4
	NH-μClay	5	3
Physical–chemical	H-μSilt	3	5
	H-μClay	4	4
Chemical	H-dSilt	1	7
	H-dClay	3	5
Biochemical	NH-dSilt	4	4
	NH-dClay	4	4

† cPOM, coarse unprotected particulate organic matter (>250 μm); μagg, microaggregate fraction (53–250 μm); LF, fine unprotected POM (lighter than 1.85 g cm^{-3}, 53–250 μm); iPOM, microaggregate-protected POM (heavier than 1.85 g cm^{-3}, >53 μm in size); NH-dSilt, nonhydrolyzable easily dispersed silt-sized fraction (acid resistant, 53–2 μm); NH-dClay, nonhydrolyzable easily dispersed clay-sized fraction (acid resistant, <2 μm); NH-μSilt, nonhydrolyzable microaggregate-derived silt-sized fraction (acid resistant, 53–2 μm); NH-μClay, nonhydrolyzable microaggregate-derived clay-sized fraction (acid resistant, <2 μm); H-dSilt, hydrolyzable easily dispersed silt-sized fraction (acid soluble, 53–2 μm); H-dClay, hy drolyzable easily dispersed clay-sized fraction (acid soluble, <2 μm); H-μSilt, hydrolyzable microaggregate-derived silt-sized fraction (acid soluble, 53–2 μm); H-μClay, hydrolyzable microaggregate-derived clay-sized fraction (acid soluble, <2 μm).

‡ The two models were indistinguishable in the μagg fraction at four sites.

The number of fractions within each site fit with the C saturation model was linearly related to the maximum whole soil SOC concentration (R^2 = 0.78, P = 0.014, excluding CO). The greatest numbers of C saturation model fits were in the SCO, AB, and CO sites (Table 2). At Swift Current (SC) and SV, five and seven fractions' data fit the C saturation model the best. Data from GA, KY, and OH had three or fewer fractions best fit with the saturation model.

Since smaller sections of an asymptotic curve can appear linear when the range being observed is small, a site with a small range of SOC concentrations will not necessarily capture the full range of linear to asymptotic behaviors expected from a soil subject to C saturation (Stewart et al., 2007). Two sites with the broadest range in SOC content (AB and SCO) had similar behavior among C pools, we report the results from SCO individually as the best example for testing C saturation, as well

Table 3. Soil organic carbon (SOC) concentrations of the fractions from Scott, SK, for the 0- to 5-cm and 5- to 20-cm depth increments under grass (G), conventional tillage (CT), and no-till (NT). The microaggregate (μagg) fraction is comprised of microaggregate-protected particulate organic matter (iPOM) and mineral-associated fractions (nonhydrolyzable = NH-μSilt and NH-μClay and hydrolyzable = H-μSilt and H-μClay).

SOC pool	Isolated fraction†	0–5 cm			5–20 cm		
		G	CT	NT	G	CT	NT
		g C kg^{-1} fraction					
Unprotected	cPOM	121.3 ± 13.0	36.2 ± 5.6	44.5 ± 8.1	11.0 ± 3.8	9.3 ± 1.3	7.6 ± 1.3
	LF	150.0 ± 16.6	198.6 ± 18.6	182.2 ± 8.3	154.4 ± 106.6	213.1 ± 16.2	213.2 ± 7.1
Physical	μagg	64.9 ± 4.8	29.2 ± 2.2	32.6 ± 2.5	18.9 ± 11.6	19.6 ± 2.0	23.2 ± 2.4
	iPOM	44.1 ± 12.6	11.8 ± 1.7	21.4 ± 3.7	4.5 ± 2.4	5.0 ± 0.6	4.9 ± 1.3
Physical–biochemical	NH-μSilt	30.3 ± 2.6	26.7 ± 0.8	26.0 ± 1.0	10.5 ± 1.2	17.2 ± 1.3	15.2 ± 2.0
	NH-μClay	29.7 ± 0.3	35.4 ± 1.2	31.7 ± 0.8	15.3 ± 2.6	23.6 ± 1.3	18.9 ± 1.7
Physical–chemical	H-μSilt	19.9 ± 2.4	13.0 ± 0.7	14.4 ± 1.2	9.0 ± 1.0	7.6 ± 0.4	10.6 ± 0.8
	H-μClay	32.5 ± 0.9	27.1 ± 0.6	33.0 ± 1.8	19.3 ± 1.8	20.4 ± 0.9	21.9 ± 0.3
Chemical	H-dSilt	20.0 ± 2.1	19.6 ± 1.2	17.5 ± 0.4	7.8 ± 0.8	13.0 ± 0.5	11.4 ± 1.2
	H-dClay	38.9 ± 1.8	36.2 ± 1.1	34.1 ± 0.8	16.5 ± 1.6	23.1 ± 1.8	24.5 ± 2.0
Biochemical	NH-dSilt	17.6 ± 0.3	15.6 ± 0.2	14.9 ± 0.6	11.9 ± 1.0	11.6 ± 0.4	13.4 ± 0.5
	NH-dClay	36.6 ± 0.8	27.5 ± 0.8	28.5 ± 0.8	22.8 ± 1.0	18.2 ± 1.9	23.0 ± 1.9

† cPOM, coarse unprotected particulate organic matter (>250 μm); μagg, microaggregate fraction (53–250 μm); LF, fine unprotected POM (lighter than 1.85 g cm^{-3}, 53–250 μm); iPOM, microaggregate-protected POM (heavier than 1.85 g cm^{-3}, >53 μm in size); NH-dSilt, nonhydrolyzable easily dispersed silt-sized fraction (acid resistant, 53–2 μm); NH-dClay, nonhydrolyzable easily dispersed clay-sized fraction (acid resistant, <2 μm); NH-μSilt, nonhydrolyzable microaggregate-derived silt-sized fraction (acid resistant, 53–2 μm); NH-μClay, nonhydrolyzable microaggregate-derived clay-sized fraction (acid resistant, <2 μm); H-dSilt, hydrolyzable easily dispersed silt-sized fraction (acid soluble, 53–2 μm); H-dClay, hydrolyzable easily dispersed clay-sized fraction (acid soluble, <2 μm); H-μSilt, hydrolyzable microaggregate-derived silt-sized fraction (acid soluble, 53–2 μm); H-μClay, hydrolyzable microaggregate-derived clay-sized fraction (acid soluble, <2 μm).

as for comparing estimates of soil fraction saturation level (Γ) within fractions.

At SCO, the experimental treatments provided the broadest range of whole soil and fraction SOC concentrations (Tables 1 and 3). The fraction data comprising the unprotected C pool (cPOM and LF fractions) fit the linear model best (Table 4, Fig. 2a and 2b). The fractions comprising the chemically (H-dClay vs. H-dSilt) and biochemically protected pools (NH-dClay vs. NH-dSilt) fit the C saturation model best (Fig. 3 and 4). The fraction C saturation levels (Γ) were significantly greater for the dispersed clay-sized fraction than for the dispersed silt-sized fractions (e.g., NH-dClay vs. NH-dSilt) in both the chemically and biochemically protected C pools.

The linear and C saturation models were indistinguishable for the physically protected pool (μagg fraction) as a whole (Table 4, Fig. 2c). Lack of differentiation between the two models in the entire μagg fraction at SCO was probably due to the composite nature of the microaggregate fraction (μagg = iPOM + H-μSilt + H-μClay + NH-μSilt + NH-μClay) and the distinct behavior of the POM vs. the mineral-associated fractions. The physically protected iPOM fraction fit the linear model best (Table 4, Fig. 5a),

Table 4. Model fit statistics for the linear model and model fit statistics and parameter estimates for the saturation model between whole soil organic carbon (SOC) and fraction organic C concentrations for each isolated fraction from the Scott, SK, samples. No parameter estimates are available (n/a) for fractions with linear best-fit. The microaggregate (μagg) fraction is comprised of microaggregate-protected particulate organic matter (iPOM) and mineral-associated fractions (non-hydrolyzable = NH-μSilt and NH-μClay and hydrolyzable = H-μSilt and H-μClay).

SOC pool	Isolated fraction†	Linear model R^2	Saturation model‡		
			R^2	ξ	Γ
					g C kg^{-1} fraction
Unprotected	cPOM	0.95	0.04	n/a§	n/a
	LF	0.14	0.06	n/a	n/a
Physical	μagg	0.96	0.96	n/a	n/a
	iPOM	0.80	0.20	n/a	n/a
Physical–biochemical	NH-μSilt	0.70	0.83	0.91 ± 0.10	55.2 ± 7.2
	NH-μClay	0.39	0.65	0.54 ± 0.10	45.3 ± 6.2
Physical–chemical	H-μSilt	0.73	0.76	1.65 ± 0.22	35.6 ± 6.4
	H-μClay	0.65	0.83	0.49 ± 0.06	42.9 ± 3.2
Chemical	H-dSilt	0.71	0.83	0.67 ± 0.07	21.1 ± 0.9
	H-dClay	0.78	0.82	0.54 ± 0.06	48.7 ± 3.8
Biochemical	NH-dSilt	0.62	0.75	1.14 ± 0.16	33.5 ± 4.4
	NH-dClay	0.65	0.80	0.54 ± 0.06	60.0 ± 5.9

† cPOM, coarse unprotected particulate organic matter (>250 μm); μagg, microaggregate fraction (53–250 μm); LF, fine unprotected POM (lighter than 1.85 g cm^{-3}, 53–250 μm); iPOM, microaggregate-protected POM (heavier than 1.85 g cm^{-3}, >53 μm in size); NH-dSilt, nonhydrolyzable easily dispersed silt-sized fraction (acid resistant, 53–2 μm); NH-dClay, nonhydrolyzable easily dispersed clay-sized fraction (acid resistant, <2 μm); NH-μSilt, nonhydrolyzable microaggregate-derived silt-sized fraction (acid resistant, 53–2 μm); NH-μClay, nonhydrolyzable microaggregate-derived clay-sized fraction (acid resistant, <2 μm); H-dSilt, hydrolyzable easily dispersed silt-sized fraction (acid soluble, 53–2 μm); H-dClay, hydrolyzable easily dispersed clay-sized fraction (acid soluble, <2 μm); H-μSilt, hydrolyzable microaggregate-derived silt-sized fraction (acid soluble, 53–2 μm); H-μClay, hydrolyzable microaggregate-derived clay-sized fraction (acid soluble, <2 μm).

‡ ξ is a scalar; Γ is the fraction C saturation limit.

§ No parameter estimates are available for fractions with linear best fit.

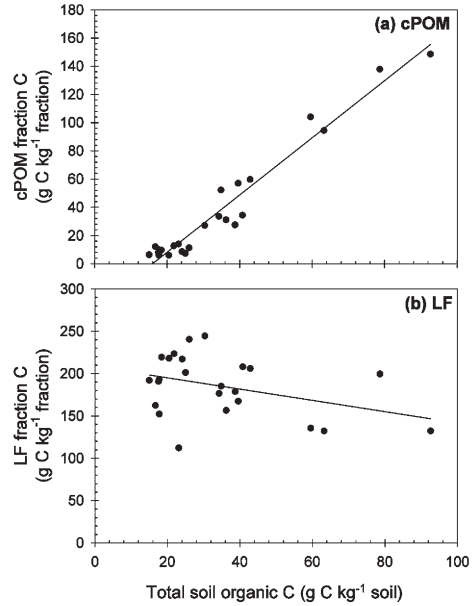

Fig. 2. Organic C concentration of the unprotected C pool, (a) coarse unprotected particulate organic matter (cPOM) and (b) fine unprotected POM (LF), isolated from the SCO (Scott, SK) samples. Lines represent the best-fit linear model for each fraction.

while the aggregate mineral-associated fractions (H-μSilt, H-μClay, NH-μSilt, and NH-μClay) fit the C saturation model best (Table 4, Fig. 5b and 5c).

Physically protected silt-sized fractions had significantly greater estimates of C saturation (Γ) than did their easily dispersed counterparts but not the clay-sized fraction (e.g., H-dClay vs. H-μClay, and NH-dClay vs. NH-μClay) (Table 4). Unlike the easily dispersed fractions, where silt- and clay-sized estimates of Γ differed, in the microaggregate-derived size fractions, Γ did not significantly differ (e.g., NH-μSilt vs. NH-μClay).

Estimates of fraction C saturation levels (Γ) for the remaining sites are only reported if the saturation model fit the data better than the linear model (Table 5). Estimates ranged from 5.9 ± 0.7 g fraction C kg^{-1} whole soil C in the NH-dSilt fraction at CO to 180 ± 20 g fraction C kg^{-1} whole soil C in the LF fraction at SC (Table 5). Of the Γ estimates whose confidence intervals did not overlap, the clay-sized fractions had greater Γ estimates than the silt-sized fractions. As was found at SCO, the microaggregate-derived silt fractions had greater estimates of Γ than the dispersed silt-sized fractions (e.g., μSilt vs. dSilt, H-μSilt vs. H-dSilt, and NH-μSilt vs. NH-dSilt).

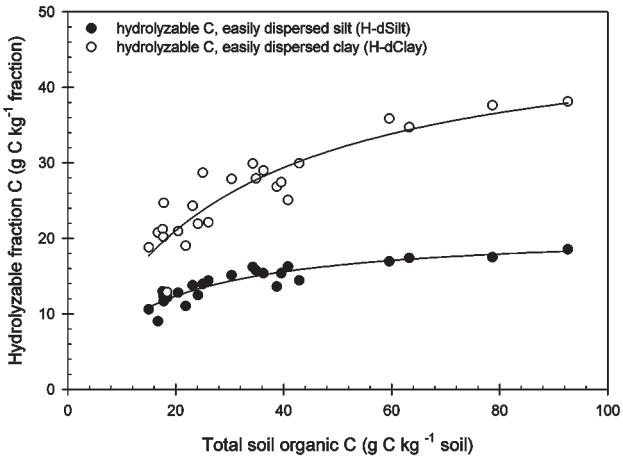

Fig. 3. Organic C concentration of the chemically protected pool isolated from the easily dispersed fractions from the SCO (Scott, SK) samples. Lines represent the best-fit C saturation model for each fraction.

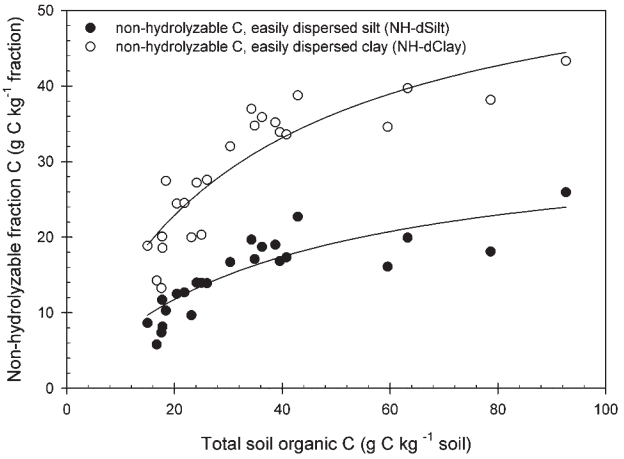

Fig. 4. Organic C concentration of the biochemically protected pools isolated from easily dispersed fractions from the SCO (Scott, SK) samples. Lines represent the best-fit C saturation model for each fraction.

All Site Data Combined

The fraction data across all sites were pooled to provide a wider range in SOC concentrations and to clarify the ambiguous results of the physically and biochemically protected C pools. The model fit results of the combined site data were similar to that of the individual site data. The chemically protected pool (H-dSilt and H-dClay) was best fit with the C saturation model and the estimate of Γ was significantly greater in the H-dClay than the H-dSilt fraction (Table 6). The fraction data of the biochemically protected pool reflected the split between models seen in the individual site data, and showed either no difference between models (NH-dSilt) or a slightly better fit with the linear model (NH-dClay) (Table 6). No best-fit model was determined in the fraction data comprising the unprotected SOC pool (cPOM). In the physically protected pool, however, the iPOM and μagg fractions fit the C saturation model better, in contrast to the individual site data, where the linear model fit best. The combined data of the mineral-associated fractions (H-μSilt, H-μClay, NH-μSilt, and NH-μClay) were split between C saturation and linear model best fits.

DISCUSSION

Ideally, saturation phenomena of specific soil fractions would be evaluated for a soil in which long-term C input rates were the sole varying factor; however, few such experiments, with a sufficiently broad range of input rates, exist (Stewart et al., 2007). We show theoretically (see Appendix) that SOC concentration can be used as a proxy for soil C input such that a linear relationship between whole SOC concentration and fraction SOC concentration indicates the lack of C saturation behavior, whereas fractions exhibiting either an asymptotic

or an exponential relationship are influenced by C saturation (Appendix). This mathematical relationship explicitly links the theory of C saturation to measurable C pools as a function of whole SOC concentration. Nevertheless, we acknowledge the limitations to this analysis imposed by using soils from different environments and with different experimental durations, which will vary in their approximation of steady-state conditions. This expression of fraction C capacity was suggested by Carter (2002), however, and it provides a feasible approach to examine soil fraction C saturation across a range of soils.

Chemically Protected Pool

The concept of a maximum limit to C storage in fractions comprising the chemically protected C pool (H-dClay and H-dSilt) is supported by the observed C saturation best-fit models at the majority of the individual sites as well as for the combined site data set. These results corroborate previous work demonstrating silt + clay protective capacity for soil C (Carter et al., 2003; Hassink, 1997; Jolivet et al., 2003; Six et al., 2002), but also illustrate distinct C saturation behavior for the silt- vs. clay-sized fractions.

Few studies have quantified clay saturation, but our estimates at individual sites ranged from 4.87 to 8.40 g C kg^{-1} clay (H-dClay fraction). Our estimates are smaller than those of the whole soil saturation constant for the temperate sandy soils (19–55 g C kg^{-1} clay) of Hassink and Whitmore (1997), and also smaller than clay saturation estimates from tropical systems of 48.8 g C kg^{-1} clay (Diekow et al., 2005) and 32.5 g C g kg^{-1} clay (Roscoe et al., 2001). The discrepancy is probably due to differences in fraction isolation methods. Diekow et al. (2005) and Roscoe et al. (2001) used complete dispersion of the soil by sonication, whereas we used the hyrolyzable fraction of the dispersed clay fraction (H-dClay), which excludes clay C retained as silt-sized and microaggregate fractions as well as the biochemically protected C (NH-dClay).

Our estimates of C saturation capacity were varied in soils that should have had similar theoretical values, given their texture and mineralogy (i.e., the three sites from Saskatchewan—SCO, SV, and SC). This could be due to the extrapolation of an asymptote from the linear portion of the data set. Both SC and SV have half the SOC content range as SCO, and consequently the C saturation model fit may have been overestimated Γ. The mechanism of SOC stabilization in this pool could be due to other factors in addition to mineralogy, however, and our values of fraction C saturation (Γ) should be considered an approximation and not definitive. Previous estimates of the influence of mineralogy on mineral SOC stabilization have been mixed. Although Hassink et al. (1997) found no differences in silt + clay SOC protection due to mineralogy, Six et al. (2002) found that silt- and clay-associated C of 1:1 dominated soils was significantly less than that of 2:1 soils and attributed this difference in C stabilization mainly to clay type.

Saturation of the chemically protected C pool is dictated by texture and mineralogy. Greater SOM protection in finer textured soils is correlated with greater C content in the silt + clay fractions for soils with greatly differing mineralogy (Carter et al., 1997; Hassink, 1997; Six et al., 2002). The linear relationship was significantly different for cultivated, grassland, and forest silt + clay fractions (0–53 μm) (Six et al., 2002) and

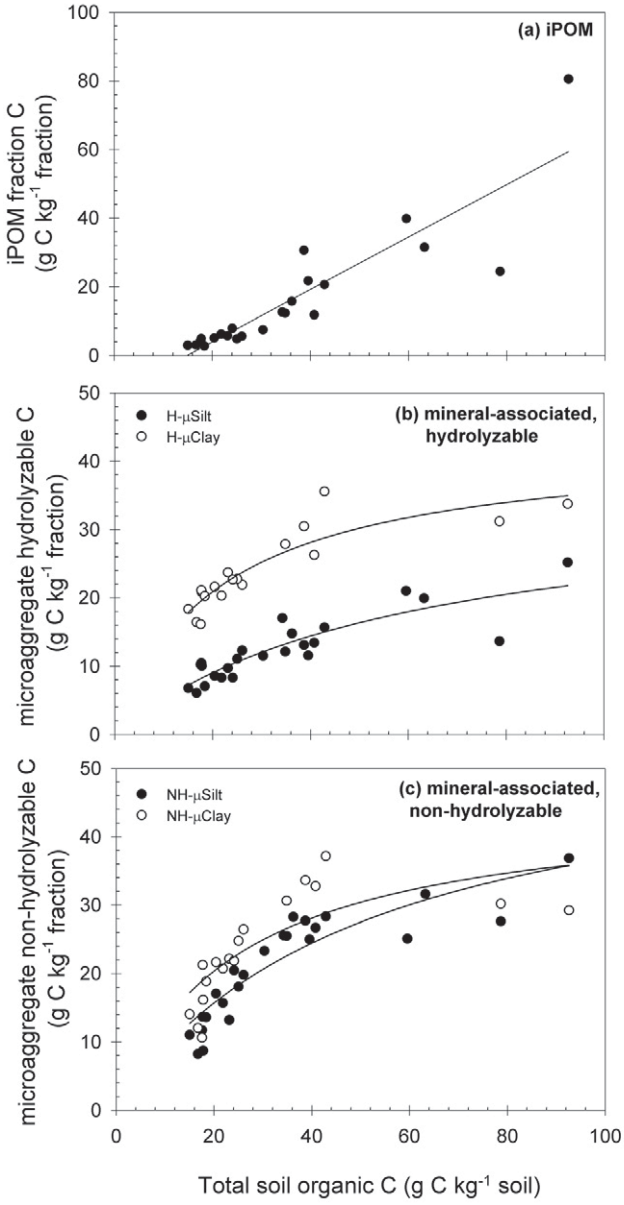

Fig. 5. Organic C concentration of the physically protected pool isolated from the SCO (Scott, SK) samples. Physically protected C consisted of (a) the microaggregate-protected particulate organic matter (iPOM) fraction and (b) mineral-associated hydrolyzable fractions (microaggregate-derived silt-sized [H-μSilt] and clay-sized [H-μClay] fractions) and (c) mineral-associated nonhydrolyzable fractions (microaggregate-derived silt-sized [NH-μSilt] and clay-sized [NH-μClay] fractions).

was probably due to differences in disturbance and C input. Hassink and Whitmore (1997) found that estimates of protective capacity were linearly related to the quantity of clay particles. We also found that estimates of C saturation of both the silt and clay fractions (Γ) were positively related to the silt + clay content of the soil (P = 0.032, R^2 = 0.82 for silt, and P = 0.027, R^2 = 0.84 for clay), suggesting a direct relationship between clay content and C sequestration capacity.

Biochemically Protected Pool

While data for fractions comprising the biochemically protected C pool for half of the individual sites fit the C saturation model best (Table 4), the combined site data fit the linear model best (Table 5). These results suggest that biochemically

Table 5. Parameter estimates and standard errors for fraction C saturation level (Γ) of the fractions best-fit C saturation model at eight long-term agroecosystem sites: Breton, AB (AB); Akron, CO (CO); Watkinsville, GA (GA); Lexington, KY (KY); Hoytville, OH (OH); Swift Current, SK (SC); Scott, SK (SCO); and Stewart Valley, SK (SV). The microaggregate (μagg) fraction is comprised of microaggregate-protected particulate organic matter (iPOM) and mineral-associated fractions (nonhydrolyzable = NH-μSilt and NH-μClay and hydrolyzable = H-μSilt and H-μClay).

SOC pool	Isolated fraction†	AB	CO	GA	KY	OH	SC	SCO	SV
		g C kg^{-1} fraction							
Unprotected	cPOM	n/a‡	n/a	n/a	n/a	n/a	n/a	n/a	n/a
	LF	n/a	n/a	n/a	n/a	n/a	180 ± 20	n/a	169 ± 24
Physical	μagg	n/a	n/a	n/a	n/a	n/a	n/a	n/a	n/a
	iPOM	n/a	n/a	n/a	n/a	n/a	n/a	n/a	n/a
Physical–biochemical	NH-μSilt	142 ± 27	11 ± 2	18 ± 6	n/a	n/a	n/a	55 ± 7	n/a
	NH-μClay	n/a	35 ± 7	n/a	14 ± 4	n/a	n/a	45 ± 6	n/a
Physical–chemical	H-μSilt	65 ± 18	n/a	n/a	n/a	51 ± 16	n/a	36 ± 6	16 ± 7
	H-μClay	n/a	47 ± 6	n/a	21 ± 6	n/a	n/a	43 ±3	n/a
Chemical	H-dSilt	21 ± 2	15 ± 4	n/a	n/a	103 ± 25	24 ± 15	21 ± 1	13 ± 4
	H-dClay	53 ± 6	n/a	n/a	n/a	84 ± 11	58 ± 13	49 ± 3	n/a
Biochemical	NH-dSilt	34 ± 4	6 ± 0	n/a	n/a	n/a	67 ±0	34 ± 4	n/a
	NH-dClay	96 ± 15	29 ± 5	n/a	n/a	n/a	n/a	60 ± 6	15 ± 4

† cPOM, coarse unprotected particulate organic matter (>250 μm); μagg, microaggregate fraction (53–250 μm); LF, fine unprotected POM (lighter than 1.85 g cm^{-3}, 53–250 μm); iPOM, microaggregate-protected POM (heavier than 1.85 g cm^{-3}, >53 μm in size); NH-dSilt, nonhydrolyzable easily dispersed silt-sized fraction (acid resistant, 53–2 μm); NH-dClay, nonhydrolyzable easily dispersed clay-sized fraction (acid resistant, <2 μm); NH-μSilt, nonhydrolyzable microaggregate-derived silt-sized fraction (acid resistant, 53–2 μm); NH-μClay, nonhydrolyzable microaggregate-derived clay-sized fraction (acid resistant, <2 μm); H-dSilt, hydrolyzable easily dispersed silt-sized fraction (acid-soluble, 53–2 μm); H-dClay, hydrolyzable easily dispersed clay-sized fraction (acid-soluble, <2 μm); H-μSilt, hydrolyzable microaggregate-derived silt-sized fraction (acid soluble, 53–2 μm); H-μClay, hydrolyzable microaggregate-derived clay-sized fraction (acid soluble, <2 μm).

‡ No parameter estimates are available for fractions with linear best fit.

protected fractions could be influenced by C saturation but only under some conditions.

Biochemical protection is acquired through condensation and complexation reactions or through the inherent complex biochemical nature of the material (Six et al., 2002). According to this definition, biochemically protected C associated with silt and clay particles would be expected to reach a saturation level. Biochemically recalcitrant materials such as charcoal may not interact with clay or silt particles, however, and would therefore be independent of the C saturation mechanisms. Our biochemically protected fractions showed evidence of C saturation at some sites, suggesting that biochemically recalcitrant plant-derived material rather than charcoal dominated the behavior of the biochemically protected C pool at those sites.

We found that, unlike the chemically protected pool, estimates of Γ for the biochemically protected pool of both the silt- and clay-sized fractions were not related to soil texture (data not shown), suggesting that biochemical saturation is independent from the chemical (silt + clay) protection mechanism. Plante et al. (2006b) also found that texture did not influence the proportion of nonhydrolyzable organic matter within silt- and clay-sized fractions. They did note a greater susceptibility of the clay- compared with the silt-sized fraction to hydrolyze, which they attributed to differences in biochemical composition between the two fractions. Carbohydrate concentrations are greater in clay-sized fractions than in silt-sized fractions (Amelung et al., 1999; Guggenberger et al., 1994; Kiem and Kogel-Knabner, 2003) and could account for differences in hydrolyzability between the two fractions.

Physically Protected Pool

Lack of model differentiation in the μagg fraction was probably due to the competing behavior of POM and mineral-associated fractions in this composite pool. The iPOM fraction had linear behavior, while the mineral-associated fractions were fit with the C saturation and linear models. This behavior is exemplified by the SCO data. It is possible that even though there was a large range of whole SOC concentrations, the capacity of this fraction to saturate was only beginning to be approached. Stewart et al. (2007) found that C saturation required a broad range of C inputs to elicit C saturation behavior and C accumulation appeared to be linear across shorter segments of a C saturation curve.

The μagg C pool was comprised of 12 to 30% iPOM C, and the remaining 60 to 75% C was mineral associated (H-μSilt + H-μClay + NH-μSilt + NH-μClay). Although physical protection of POM has been proposed as a process of C stabilization in microaggregates (Six et al., 2002), this mechanism appears to be less important than the chemical stabilization of non-POM by silt and clay binding in determining μagg C content (Denef et al., 2004). The linear, nonsaturating behavior of the iPOM, compared with the asymptotic, saturating behavior of the aggregate mineral-associated fractions (H-μSilt + H-μClay + NH-μSilt + NH-μClay), suggests that microaggregate silt- and clay-associated C will saturate before iPOM.

Although the model fits suggest nonsaturating behavior for the μagg pool, there should be a limit for the μagg pool based on the clay content of the soil as well as the type of clay available to protect POM (Six et al., 2002). We found that the total microaggregate mass does appear to reach a maximum level as clay content increases, suggesting that C accumulation in this fraction is indeed limited by soil texture ($P = 0.005$, $R^2 = 0.23$) Koelbl and Kogel-Knabner (2004) also found a curvilinear relationship between clay content and occluded POM C, suggesting a maximum amount of physical protection of POM.

Unprotected Pool

Across the range of C concentrations we examined, the linear behavior of the unprotected pool for both the combined and individual site data did not support the hypothesis of C saturation in this pool. The cPOM fractions from the majority of individual sites as well as the combined site data fit the linear model best. In the LF portion of this pool, the negative relationship between whole SOC concentration and fraction C concentration was unexpected, and may reflect incorporation of LF into aggregate structures or mineral association with the fraction at greater C concentrations. This finding is also contrary to the previous suggestions of C saturation of the unprotected pool by Six et al. (2002). They found that despite increasing C inputs, LF C did not increase at Melfort, SK (data from Janzen et al. [1992] and Campbell et al. [1991]). Additionally, LF C did not increase in a study by Solberg et al. (1997) over increasing productivity through N fertilizer applications (25, 50, and 75 kg ha^{-1}).

The unprotected pool proposed by Six et al. (2002) consisted of plant residues, fungal hyphae and spores, and in some cases charcoal. The plant-derived nature of this pool has been verified visually, as well as through biochemical characterization (e.g., low carbohydrate and high lignin concentration). The hypothetical saturation behavior of the unprotected C pool is independent of the other protection mechanisms and is determined by the balance between C input through plant production and the specific decomposition rate of the pool. Thus, controls on microbial activity such as soil temperature, moisture, substrate biodegradability, and N availability would influence C storage in this pool.

Table 6. Model fit statistics for the linear model and model fit statistics and parameter estimates for the saturation model between whole soil organic carbon (SOC) and fraction organic C concentrations for each isolated fraction from the combined site data. No parameter estimates available for fractions with linear best-fit. The microaggregate (μagg) fraction is comprised of microaggregate-protected particulate organic matter (iPOM) and mineral-associated fractions (non-hydrolyzable = NH-μSilt and NH-μClay and hydrolyzable = H-μSilt and H-μClay).

SOC Pool	Isolated fraction†	Linear model R^2	Saturation model		
			R^2	ξ‡	Γ
					g C kg^{-1} fraction
Unprotected	cPOM	0.60	0.60	n/a§	n/a
	LF¶	–	–	–	–
Physical	μagg	0.87	0.88	0.93 ± 0.03	458.7 ± 116.9
	iPOM	0.09	0.10	0.79 ± 0.17	84.5 ± 38.4
Physical–biochemical	NH-μSilt	0.75	0.75	n/a	n/a
	NH-μClay	0.52	0.52	n/a	n/a
Physical–chemical	H-μSilt	0.44	0.50	1.54 ± 0.11	41.7 ± 6.0
	H-μClay	0.39	0.37	n/a	n/a
Chemical	H-dSilt	0.59	0.65	1.59 ± 0.08	33.0 ± 3.0
	H-dClay	0.39	0.65	0.91 ± 0.05	52.1 ± 4.3
Biochemical	NH-dSilt	0.63	0.63	n/a	n/a
	NH-dClay	0.65	0.64	n/a	n/a

† cPOM, coarse unprotected particulate organic matter (>250 μm); μagg, microaggregate fraction (53–250 μm); LF, fine unprotected POM (lighter than 1.85 g cm^{-3}, 53–250 μm); iPOM, microaggregate-protected POM (heavier than 1.85 g cm^{-3}, >53 μm in size); NH-dSilt, nonhydrolyzable easily dispersed silt-sized fraction (acid resistant, 53–2 μm); NH-dClay, nonhydrolyzable easily dispersed clay-sized fraction (acid resistant, <2 μm); NH-μSilt, nonhydrolyzable microaggregate-derived silt-sized fraction (acid resistant, 53–2 μm); NH-μClay, nonhydrolyzable microaggregate-derived clay-sized fraction (acid resistant, <2 μm); H-dSilt, hydrolyzable easily dispersed silt-sized fraction (acid soluble, 53–2 μm); H-dClay, hydrolyzable easily dispersed clay-sized fraction (acid soluble, <2 μm); H-μSilt, hydrolyzable microaggregate-derived silt-sized fraction (acid soluble, 53–2 μm); H-μClay, hydrolyzable microaggregate-derived clay-sized fraction (acid soluble, <2 μm).

‡ ξ is a scalar; Γ is the fraction C saturation limit.

§ No parameter estimates are available for fractions with linear best fit.

¶ Due to the significant relationship between decomposition constant ξ (estimated from the linear model fit) and average SOC concentration (C_t), we do not report the model fit for the LF due to possible confounding factors of the analysis.

CONCLUSIONS

The expression of C saturation may be expanded from whole SOC as a function of C inputs to individual soil fractions evaluated across whole SOC concentration. From mathematical derivations of simple contrasting decomposition models (Stewart et al., 2007), we showed that fractions having a linear relationship between C input and SOC at steady state also express a linear relationship between fraction and whole SOC concentration. We found that fraction C saturation may be expressed as either an asymptotic or exponential relationship as a function of whole SOC concentration. These simple expressions were used to evaluate measurable fractions corresponding to free POM (unprotected), microaggregate-associated C (physically protected), silt- and clay-associated C (chemically protected), and nonhydrolyzable C (biochemically protected) fractions. The microaggregate-associated fraction was further fractioned to assess mineral-associated vs. POM C stabilization.

In the eight long-term agroecosystem experiments across the United States and Canada, the number of fractions fitting the C saturation model within each site was directly related to maximum SOC content. The two sites with the greatest SOC range showed C saturation behavior in the chemically and biochemically protected pools, as well as the mineral-associated physically protected pool. These results indicate the importance of including biochemical and physical C protection in fractionation schemes. In contrast, the unprotected C pool and the POM-associated microaggregate C pool showed linear, nonsaturating behavior.

The majority of the remaining sites and the combined site data showed C saturation behavior in the chemically protected C pool. At the individual sites, the biochemical pool was split between C saturation and linear model fits, but showed no evidence of C saturation when the data were combined. The physically protected pool also showed support for C saturation in the combined site data, but the individual site data fit the linear model best. This was probably due to the composite nature of the physically protected pool, comprised of POM

and mineral-associated C. The unprotected pool showed primarily linear best-model fits.

Carbon saturation was observed in soil fractions from a variety of soil taxonomies, textures, and climates, suggesting that C of the chemically as well as the biochemically protected pools is influenced by C saturation behavior even though the whole soil may not be saturated with respect to C. If the chemically protected pool is filled, further accumulation of C will probably occur in aggregate and unprotected fractions. This C is inherently less stable and subject to increased decomposition due to changes in management.

APPENDIX

Soil C saturation has previously been expressed as an asymptotic relationship between whole SOC and C inputs at steady state (Six et al., 2002; Stewart et al., 2007). In the current analysis, we sought to express C saturation of individual soil fractions. This requires a normalized scale because differing treatments will result in differing rates of decomposition and incorporation of C input into various C pools as well as transfers among them. Whole SOC concentration, as a balance between C input and decomposition, normalizes the fraction data across treatments. To express C saturation as a function of SOC concentration rather than soil C input requires determining the mathematical relationship between the C concentrations of individual soil fractions and total SOC concentration.

Stewart et al. (2007) previously described two simple models of SOC accumulation with respect to C input. The first was a single-pool model that assumed no C saturation limit (i.e., a linear response of steady-state SOC). The linear model assumed that residue C transformed into SOC was independent of pool size and that decomposition rates are directly proportional to the pool size. At steady-state,

$$C_t^* = \frac{I^*}{k} + R \qquad [A1]$$

SOC content (C_t^*) is directly proportional to C inputs (I^*), where k is the specific decay constant. An intercept term (R) was added to the linear model in Eq. [A1] to account for the residual SOC that is not affected during the course of an agroecosystem experiment.

The second model was a single-pool model, but assumed whole soil C saturation (i.e., asymptotic steady-state SOC). In the C saturation model, soil organic C accumulation was limited by the soil's saturation deficit (sd), or how far away from C saturation (C_m) a soil is:

$$\mathrm{sd} = 1 - \frac{C_t^*}{C_m} \qquad [A2]$$

which results in an asymptotic relationship between C inputs (I^*) and SOC concentration (C_t^*) at steady state:

$$C_t^* = \frac{I^*}{k + (I^*/C_m)} \qquad [A3]$$

To derive the mathematical relationship between the C concentration of individual soil fractions and total SOC concentration, rather than with respect to C inputs as previously reported (Stewart et al., 2007; Six et al., 2002), we constructed two hypothetical model scenarios in which the whole soil is comprised of two pools (e.g., active and passive) either having linear C accumulation as a function of C inputs, or asymptotic C accumulation as a function of C inputs in accordance with the C saturation concept. Using these two hypothetical cases, we solved for each C pool with respect to total SOC concentration to determine if C saturation can be expressed as a function of total SOC concentration.

At steady state, the two-pool model for whole soil C concentration is:

$$C_t^* S = C_1^* S(m_1) + C_2^* S(1 - m_1) \qquad [A4]$$

where C_1 is the C concentration in Pool 1 (kg C kg^{-1} Fraction 1), C_2 is the C concentration in Pool 2 (kg C kg^{-1} Fraction 2), m_1 is the mass proportion of Fraction 1 in the whole soil (kg Fraction 1 kg^{-1} soil), S is the mass of whole soil (e.g., g soil), and C_t is the C concentration in the whole soil (kg C kg^{-1} soil).

In the linear case, each pool is directly related to C input

$$C_1^* S(m_1) = \frac{I^* p_1}{k_1} \qquad [A5]$$

$$C_2^* S(1 - m_1) = \frac{I^*(1 - p_1)}{k_2} \qquad [A6]$$

where p_1 and $1 - p_1$ are the proportion of C input (I^*) partitioned to pools C_1^* and C_2^*, and k_1 and k_2 are the decomposition rates of each pool. To express C_1^* as a function of C_t, we isolated I^* in Eq. [A5], and C_2^* in Eq. [A6], and substituted the solution of I^* into the solution for C_2^*. The resulting equation for C_2^* was substituted into Eq. [A4] and solved in terms of C_1^* to obtain

$$C_1^* = \frac{p_1 k_2}{m_1 \left[p_1 k_2 + k_1 (1 - p_1) \right]} C_t^* \qquad [A7]$$

To express the C concentration of the second pool (C_2^*) as a function of C_t, we substituted the solution of C_1^* (Eq. [A7]) for C_1^* in Eq. [A4] and solved for C_2^*:

$$C_2^* = \frac{k_1 (1 - p_1)}{(1 - m_1)\left[p_1 k_2 + k_1 (1 - p_1) \right]} C_t^* \qquad [A8]$$

The resultant expression shows that fraction C concentrations (C_1^* and C_2^*) are a linear function of whole SOC concentration (C_t^*), and are dependent on the proportion of C input of both pools, their mass proportions, and their decomposition constants. These expressions can also be reduced to a simple linear equation:

$$C_f^* = \omega C_t^* + R \qquad [A9]$$

where ω is the aggregate of the constants in Eq. [A7] or [A8] and R is an intercept term to account for residual SOC that is not affected during the course of an agroecosystem experiment.

In the C saturation case, C concentrations in each fraction are asymptotic with respect to C input at steady state:

$$C_1^* S(m_1) = \frac{I^* p_1}{k_1 + (I^* p_1 / C_{m1})} \qquad [A10]$$

$$C_2^* S(1 - m_1) = \frac{I^*(1 - p_1)}{k_2 + \left[I^*(1 - p_1) / C_{m2} \right]} \qquad [A11]$$

where C_{m1} and C_{m2} are the saturation limits of each fraction.

As for the linear case above, solving Eq. [A10] and [A11] to express C_1^* and C_2^* in terms of C_t yields the following by grouping constants (represented by α, β, and γ):

$$C_1^* = \frac{\alpha C_t - \beta \pm \sqrt{\alpha^2 C_t^2 - \gamma C_t + \beta^2}}{-2\alpha m_1} \quad [A12]$$

$$\alpha = S\left(k_2 C m_2 p_1 - k_1 C m_1 + k_1 C m_1 p_1\right)$$

$$\beta = C m_1 C m_2 \left(k_1 + k_2 p_2 - k_1 p_1\right)$$

$$\gamma = -2SC m_1 C m_2 \left(-k_1 + k_2 p_2 + k_1 p_1\right)\left(k_2 C m_2 p_1 - k_1 C m_1 + k_1 C m_1 p_1\right)$$

Solving for the second pool (C_2*) and grouping variables (represented by α, β, and γ),

$$C_2^* = \frac{-\alpha C_t + \beta \pm \sqrt{(-\alpha)^2 C_t^2 - \gamma C_t + \beta^2}}{-2\alpha\left(1 - m_1\right)} \quad [A13]$$

$$\alpha = S\left(k_2 C m_2 p_1 - k_1 C m_1 + k_1 C m_1 p_1\right)$$

$$\beta = C m_1 C m_2 \left(k_1 + k_2 p_2 - k_1 p_1\right)$$

$$\gamma = 2SC m_1 C m_2 \left(-k_1 + k_2 p_2 + k_1 p_1\right)\left(k_2 C m_2 p_1 - k_1 C m_1 + k_1 C m_1 p_1\right)$$

Although there are two solutions for each pool, only the solutions in positive space are relevant. We took the limit of each solution as whole soil C content approached infinity to ascertain the behavior of each pool. The limit of the first pool is an asymptote, $C_1^* = \beta/2\alpha m_1$, while at the limit the other pool increases linearly with respect to total organic C, $C_2^* = C_t/(1 - m_1)$. Since the first and second pools must sum to C_t, as one approaches an asymptotic limit the other fraction has an upwardly increasing slope with respect to whole soil C concentration, declining to a linear (constant slope) relationship in the limit (Fig. A1b). Both relationships have been observed by Diekow et al. (2005) with the asymptotic pool corresponding to the clay-associated C and an increasing exponential relationship for the sand-sized fraction (Fig. A1a). Therefore, C pools that are asymptotic with respect to soil C inputs (i.e., saturated) can also have an asymptotic relationship between fraction C and whole SOC concentration. For our modeling purposes, we used a simple asymptotic equation:

$$C_f^* = \frac{C_t^*}{\xi + \left(C_t^*/\Gamma\right)} \quad [A14]$$

that allowed us to explicitly estimate a maximum amount of C in the fraction (i.e., the limit in Eq. [A12]) with a single parameter (Γ), rather than the three parameters above. It is important to note that given this expression, a linear relationship between fraction C content and SOC content is not a direct refutation of C saturation, as the difference between an increasing exponential curve (C_{f2} in Fig. A1) and a linear curve may not be evident. We cannot assess whole soil C saturation on the basis of multiple fraction behavior.

With this derivation, we have demonstrated that SOC concentration may be used as a proxy for soil C input in our analysis. We hypothesize that a measured soil fraction exhibiting a linear relationship between whole SOC concentration and fraction SOC concentration is not influenced by C saturation, while a fraction exhibiting an asymptotic relationship is influenced by C saturation. Since we are concerned only with the general relationship between SOC and fraction C, simple mathematical expressions of both relationships will suffice (Eq. [A9] and [A14]).

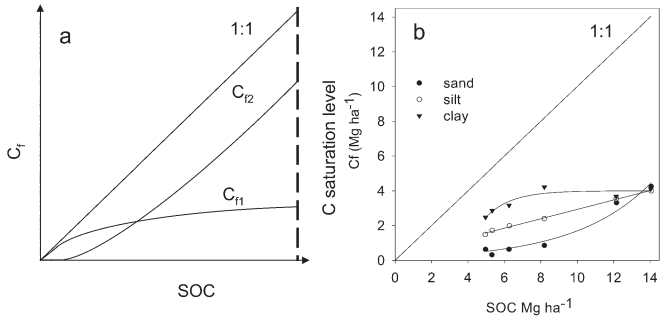

Fig. A1. (a) Theoretical behavior of two C pools under assumptions of C saturation. One pool demonstrates asymptotic behavior (C_{f1}), while the other has an upward exponential behavior (C_{f2}). Both pools sum to the 1:1 line representing soil organic carbon (SOC)/SOC. Under conditions of C saturation, whole-soil SOC does not increase and neither does fraction SOC. In this case, both fractions have reached a C saturation limit, although one demonstrates increasing exponential and the other asymptotic behavior in the whole soil. (b) Both asymptotic and upward exponential C saturation behavior are evident in the measured clay and sand fractions of Diekow et al. (2005) in the 0- to 2.5-cm depth of a subtropical Acrisol. Silt demonstrates linear C accumulation behavior.

ACKNOWLEDGMENTS

We wish to thank Dr. Donald Estep, Program for Interdisciplinary Mathematics, Ecology, and Statistics, and Dr. Jim Graham for mathematical assistance, and Gabriella Bucini and Gabe Olchin for many helpful modeling discussions. We wish to thank Alberta Agriculture, Food and Rural Development (Alberta), Merle Vigil and the USDA-ARS Central Great Plains Research Station (Colorado), Alan Franzluebbers at the USDA-ARS Natural Resource Conservation Center (Georgia), Edmund Perfect at the University of Kentucky and the Kentucky Agricultural Experiment Station (Kentucky), Matthew Davis and the Ohio Agricultural Research and Development Center's Northwest Agricultural Research Station (Ohio), and Brian McConkey and Agriculture and Agri-Food Canada (Swift Current, Scott, and Stewart Valley, Saskatchewan) for permission to sample as well as the maintenance of the long-term field experiments. We would also like to acknowledge Dick Puurveen (Alberta), Linda Hardesty and Jean-Marie Pouppirt (Colorado), Frank Thayer, Nathan David, and Jeannette Durkalski (Ohio), and Kelsey Brandt (Swift Current, Scott, and Stewart Valley, Saskatchewan) for field assistance during sampling. We thank Karolien Denef for sampling Kentucky. Laboratory assistance during the soil fractionations and acid hydrolysis was provided by Jodi Stevens, Mike Katz, Shane Cochran, Sarah Moculeski, Joyce Dickens, and Colin Pinney. This project was supported by the Office of Research (BER), U.S. Department of Energy Grants DE-FG03–00ER62997, DE-FG02– 04ER63912, and DE-FG02–04ER63890, and from the Cooperative State Research, Education, and Extension Service, USDA, Grant no. 2001-38700-11092.

REFERENCES

Amelung, W., K.W. Flach, and W. Zech. 1999. Lignin in particle-size fractions of native grassland soils as influenced by climate. Soil Sci. Soc. Am. J. 63:1222–1228.

Baldock, J.A., and J.O. Skjemstad. 2000. Role of the soil matrix and minerals in protecting natural organic materials against biological attack. Org. Geochem. 31:697–710.

Brandt, S.A. 1992. Zero vs. conventional tillage and their effects on crop yield

and soil moisture. Can. J. Plant Sci. 72:679–688.
Campbell, C.A., V.O. Biederbeck, R.P. Zentner, and G.P. Lafond. 1991. Effect of crop rotations and cultural practices on soil organic matter, microbial biomass and respiration in a thin Black Chernozem. Can. J. Soil Sci. 71:363–376.
Campbell, C.A., B.G. McConkey, R.P. Zentner, F.B. Dyck, F. Selles, and D. Curtin. 1995. Carbon sequestration in a Brown Chernozem as affected by tillage and rotation. Can. J. Soil Sci. 75:449–458.
Campbell, C.A., B.G. McConkey, R.P. Zentner, F. Selles, and D. Curtin. 1996. Tillage and crop rotation effects on soil organic C and N in a coarse-textured Typic Haploboroll in southwestern Saskatchewan. Soil Tillage Res. 37:3–14.
Carter, M.R. 2002. Soil quality for sustainable land management: Organic matter and aggregation interactions that maintain soil functions. Agron. J. 94:38–47.
Carter, M.R., D.A. Angers, E.G. Gregorich, and M.A. Bolinder. 1997. Organic carbon and nitrogen stocks and storage profiles in cool, humid soils of eastern Canada. Can. J. Soil Sci. 77:205–210.
Carter, M.R., D.A. Angers, E.G. Gregorich, and M.A. Bolinder. 2003. Characterizing organic matter retention for surface soils in eastern Canada using density and particle size fractions. Can. J. Soil Sci. 83:11–23.
Denef, K., and J. Six. 2005. Clay mineralogy determines the importance of biological versus abiotic processes for macroaggregate formation and stabilization. Eur. J. Soil Sci. 56:469–479.
Denef, K., J. Six, R. Merckx, and K. Paustian. 2004. Carbon sequestration in microaggregates of no-tillage soils with different clay mineralogy. Soil Sci. Soc. Am. J. 68:1935–1944.
Dick, W., W. Edwards, and E. McCoy. 1997. Continuous application of no-tillage to Ohio soils: Changes in crop yields and organic matter-related soil properties. p. 171–182. *In* E.A. Paul et al. (ed.) Soil organic matter in temperate agroecosystems: Long-term experiments in North America. CRC Press, Boca Raton, FL.
Diekow, J., J. Mielniczuk, H. Knicker, C. Bayer, D.P. Dick, and I. Kogel-Knabner. 2005. Carbon and nitrogen stocks in physical fractions of a subtropical Acrisol as influenced by long-term no-till cropping systems and N fertilisation. Plant Soil 268:319–328.
Elliott, E.T. 1986. Aggregate structure and carbon, nitrogen, and phosphorus in native and cultivated soils. Soil Sci. Soc. Am. J. 50:627–633.
Endale, D.M., M.L. Cabrera, J.L. Steiner, D.E. Radcliffe, W.K. Vencill, H.H. Schomberg, and L. Lohr. 2002. Impact of conservation tillage and nutrient management on soil water and yield of cotton fertilized with poultry litter or ammonium nitrate in the Georgia Piedmont. Soil Tillage Res. 66:55–68.
Follett, R.F., E.A. Paul, and E.G. Pruessner. 2007. Soil carbon dynamics during a long-term incubation study involving ^{13}C and ^{14}C measurements. Soil Sci. 172:189–208.
Frye, W.W., and R. Blevins. 1997. Soil organic matter under long-term no-tillage and conventional tillage corn production in Kentucky. p. 343–351. *In* E.A. Paul et al. (ed.) Soil organic matter in temperate agroecosystems: Long-term experiments in North America. CRC Press, Boca Raton, FL.
Gee, G.W., and J.W. Bauder. 1986. Particle size analysis. p. 383–411. *In* A. Klute (ed.) Methods of soil analysis. Part 1. Physical and mineralogical methods. 2nd ed. Agron. Monogr. 9. ASA and SSSA, Madison, WI.
Guggenberger, G., B.T. Christensen, and W. Zech. 1994. Land-use effects on the composition of organic matter in particle-size separates of soil: 1. Lignin and carbohydrate signature. Eur. J. Soil Sci. 45:449–458.
Halvorson, A.D., G.A. Peterson, and C.A. Reule. 2002. Tillage system and crop rotation effects on dryland crop yields and soil carbon in the central Great Plains. Agron. J. 94:1429–1436.
Halvorson, A.D., M.F. Vigil, G.A. Peterson, and E.T. Elliot. 1997. Long-term tillage and crop residue management study at Akron, Colorado. p. 361–371. *In* E.A. Paul et al. (ed.) Soil organic matter in temperate agroecosystems: Long-term experiments in North America. CRC Press, Boca Raton, FL.
Harter, R.D., and G. Stotzky. 1971. Formation of clay–protein complexes. Soil Sci. Soc. Am. Proc. 35:383–389.
Hassink, J. 1997. The capacity of soils to preserve organic C and N by their association with clay and silt particles. Plant Soil 191:77–87.
Hassink, J., and A.P. Whitmore. 1997. A model of the physical protection of organic matter in soils. Soil Sci. Soc. Am. J. 61:131–139.
Hassink, J., A.P. Whitmore, and J. Kubat. 1997. Size and density fractionation of soil organic matter and the physical capacity of soils to protect organic matter. Eur. J. Agron. 7:189–199.
Janzen, H.H., C.A. Campbell, S.A. Brandt, G.P. Laford, and L. Townley-Smith. 1992. Light-fraction organic matter in soils from long-term crop rotations. Soil Sci. Soc. Am. J. 56:1799–1806.
Jolivet, C., D. Arrouays, J. Leveque, F. Andreux, and C. Chenu. 2003. Organic carbon dynamics in soil particle-size separates of sandy Spodosols when forest is cleared for maize cropping. Eur. J. Soil Sci. 54:257–268.
Kiem, R., and I. Kogel-Knabner. 2003. Contribution of lignin and polysaccharides to the refractory carbon pool in C-depleted arable soils. Soil Biol. Biochem. 35:101–118.
Koelbl, A., and I. Kogel-Knabner. 2004. Content and composition of free and occluded particulate organic matter in a differently textured arable Cambisol as revealed by solid-state ^{13}C NMR spectroscopy. Z. Pflanzenernahr. Bodenkd. 167:45–53.
Marshman, N.A., and K.C. Marshall. 1981. Bacterial growth on proteins in the presence of clay minerals. Soil Biol. Biochem. 13:127–134.
Nyborg, M., E.D. Solberg, S.S. Malhi, and R.C. Izaurralde. 1995. Fertilizer N, crop residue, and tillage alter soil C and N content in a decade. p. 93–100. *In* R. Lal et al. (ed.) Soil management and greenhouse effect. Adv. Soil Sci. Ser. CRC Press, Boca Raton, FL.
Paul, E.A., K. Paustian, and C.V. Cole (ed.). 1997. Soil organic matter in temperate agroecosystems: Long-term experiments in North America. CRC Press, Boca Raton, FL.
Plante, A.F., R.T. Conant, E.A. Paul, K. Paustian, and J. Six. 2006a. Acid hydrolysis of easily dispersed and microaggregate-derived silt and clay-sized fractions to isolate resistant soil organic matter. Eur. J. Soil Sci. 57:456–467.
Plante, A.F., R.T. Conant, C.E. Stewart, K. Paustian, and J. Six. 2006b. Impact of soil texture on the distribution of soil organic matter in physical and chemical fractions. Soil Sci. Soc. Am. J. 70:287–296.
Plante, A.F., C.E. Stewart, R.T. Conant, K. Paustian, and J. Six. 2006c. Soil management effects on organic carbon in isolated fractions of a Gray Luvisol. Can. J. Soil Sci. 86:141–151.
Roscoe, R., P. Buurman, E.J. Velthorst, and C.A. Vasconcellos. 2001. Soil organic matter dynamics in density and particle size fractions as revealed by the $^{13}C/^{12}C$ isotopic ratio in a Cerrado's Oxisol. Geoderma 104:185–202.
Sherrod, L.A., G. Dunn, G.A. Peterson, and R.L. Kolberg. 2002. Inorganic carbon analysis by modified pressure-calcimeter method. Soil Sci. Soc. Am. J. 66:299–305.
Six, J., R.T. Conant, E.A. Paul, and K. Paustian. 2002. Stabilization mechanisms of soil organic matter: Implications for C-saturation of soils. Plant Soil 241:155–176.
Six, J., E.T. Elliot, and K. Paustian. 2000. Soil macroaggregate turnover and microaggregate formation: A mechanism for C sequestration under no-tillage agriculture. Soil Biol. Biochem. 32:2099–2103.
Six, J., E.T. Elliot, K. Paustian, and J.W. Doran. 1998. Aggregation and soil organic matter accumulation in cultivated and native grassland soils. Soil Sci. Soc. Am. J. 62:1367–1377.
Solberg, E.D., M. Nyborg, R.C. Izaurralde, S.S. Mahli, H.H. Janzen, and M. Molina-Ayala. 1997. Carbon storage in soils under continuous cereal grain cropping: N fertilizer and straw. p. 235–213. *In* R. Lal et al. (ed.) Management of carbon sequestration in soil. CRC Press, Boca Raton, FL.
Stewart, C.E., K. Paustian, R.T. Conant, A.F. Plante, and J. Six. 2007. Soil C saturation: Concept, evidence, and evaluation. Biogeochemistry 86:19–31.